STRUCTURAL MECHANICS

RUHR UNIVERSITY BOCHUM

RUB

Real-Time Prediction of Structural Processes with Polymorphic Uncertain Data

Ba Trung Cao, Steffen Freitag and Günther Meschke

Institute for Structural Mechanics,
Collaborative Research Center (SFB 837)

Ruhr University Bochum, Germany

Content

Motivation

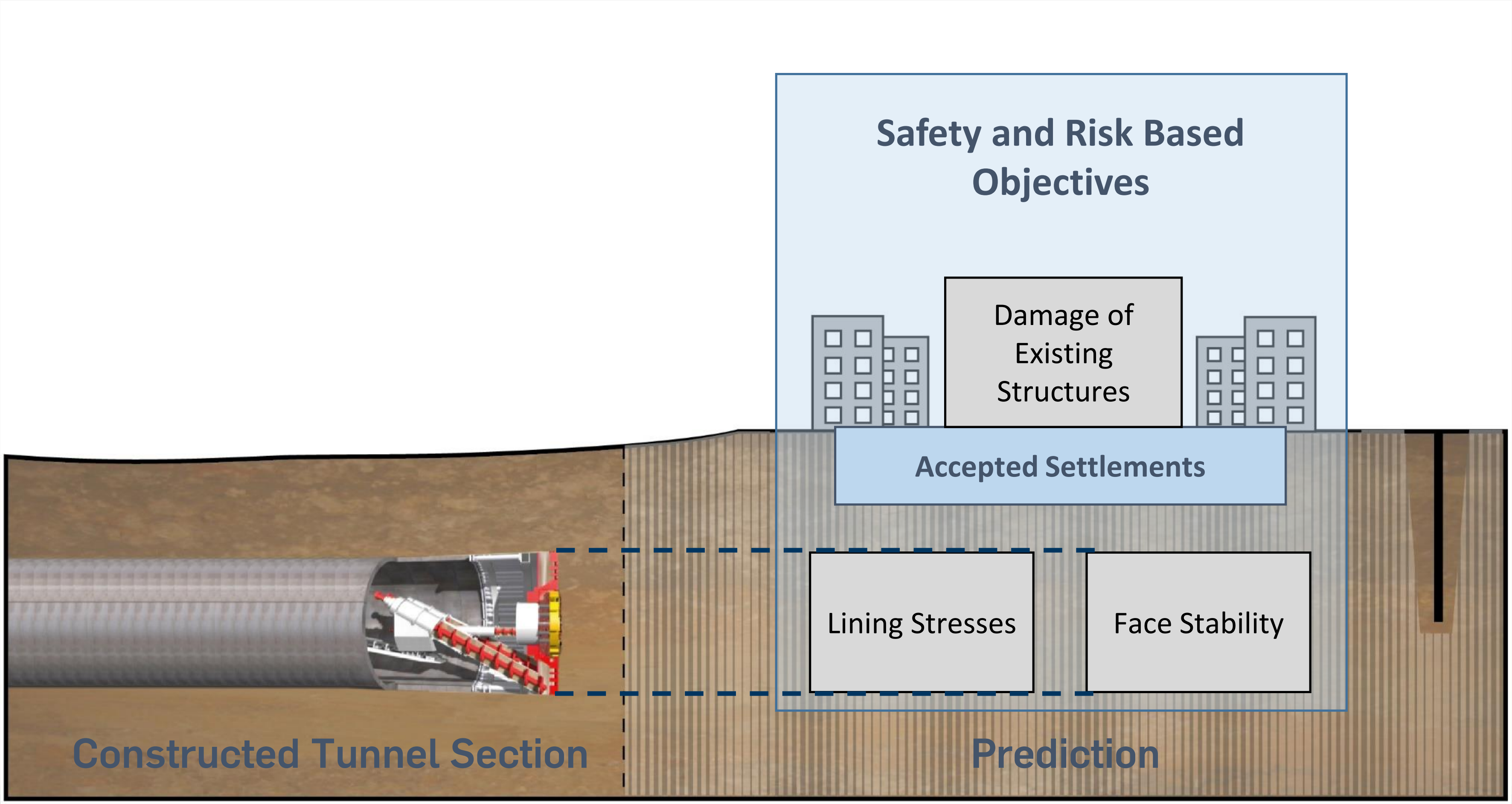
Safety and Risk Based Objectives
Damage of Existing Structures
Accepted Settlements
Lining Stresses
Face Stability
Constructed Tunnel Section
Prediction

Motivation

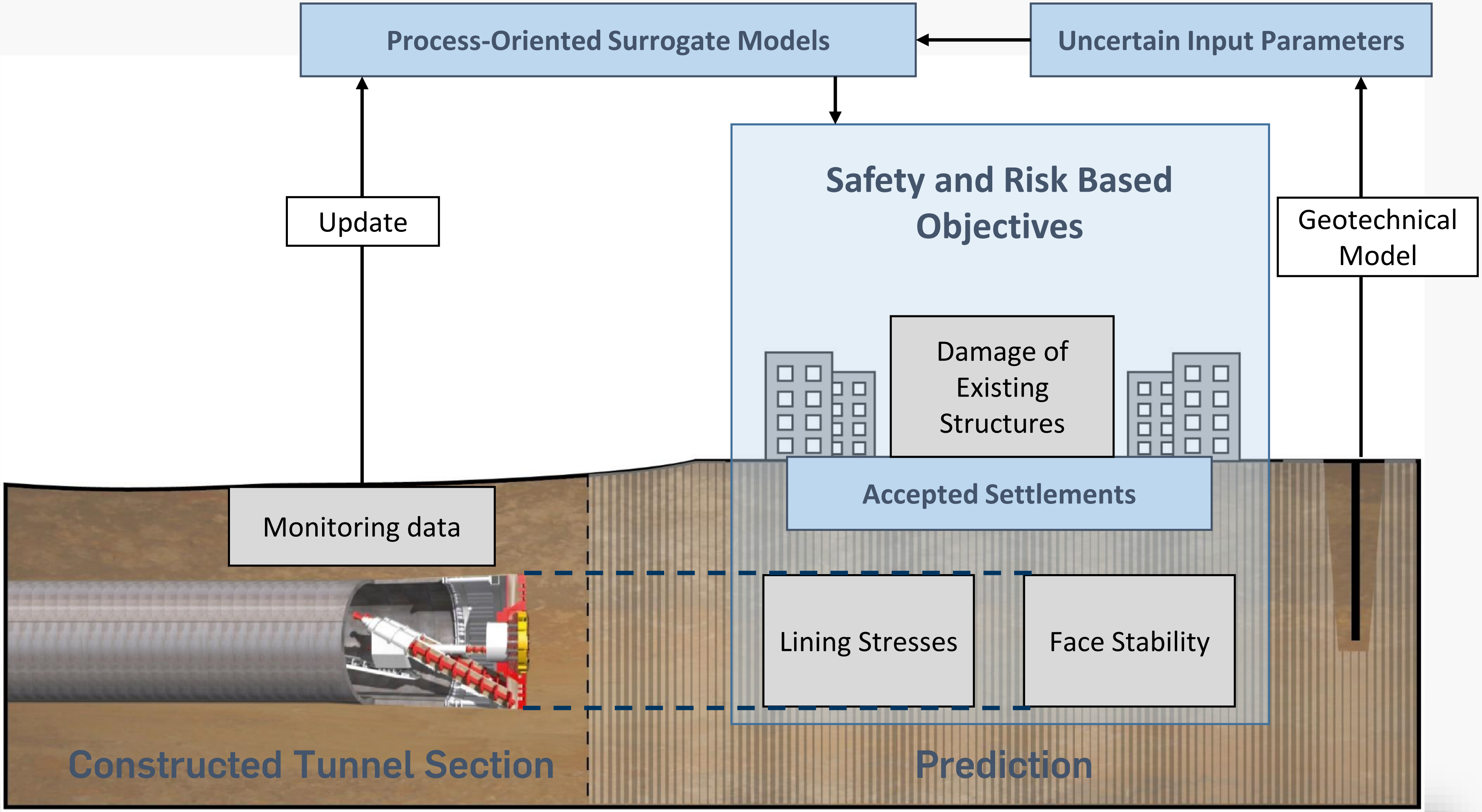
Process-Oriented Surrogate Models
Uncertain Input Parameters
Update
Safety and Risk Based Objectives
Geotechnical Model
Damage of Existing Structures
Accepted Settlements
Monitoring data
Lining Stresses
Face Stability
Constructed Tunnel Section
Prediction

Motivation

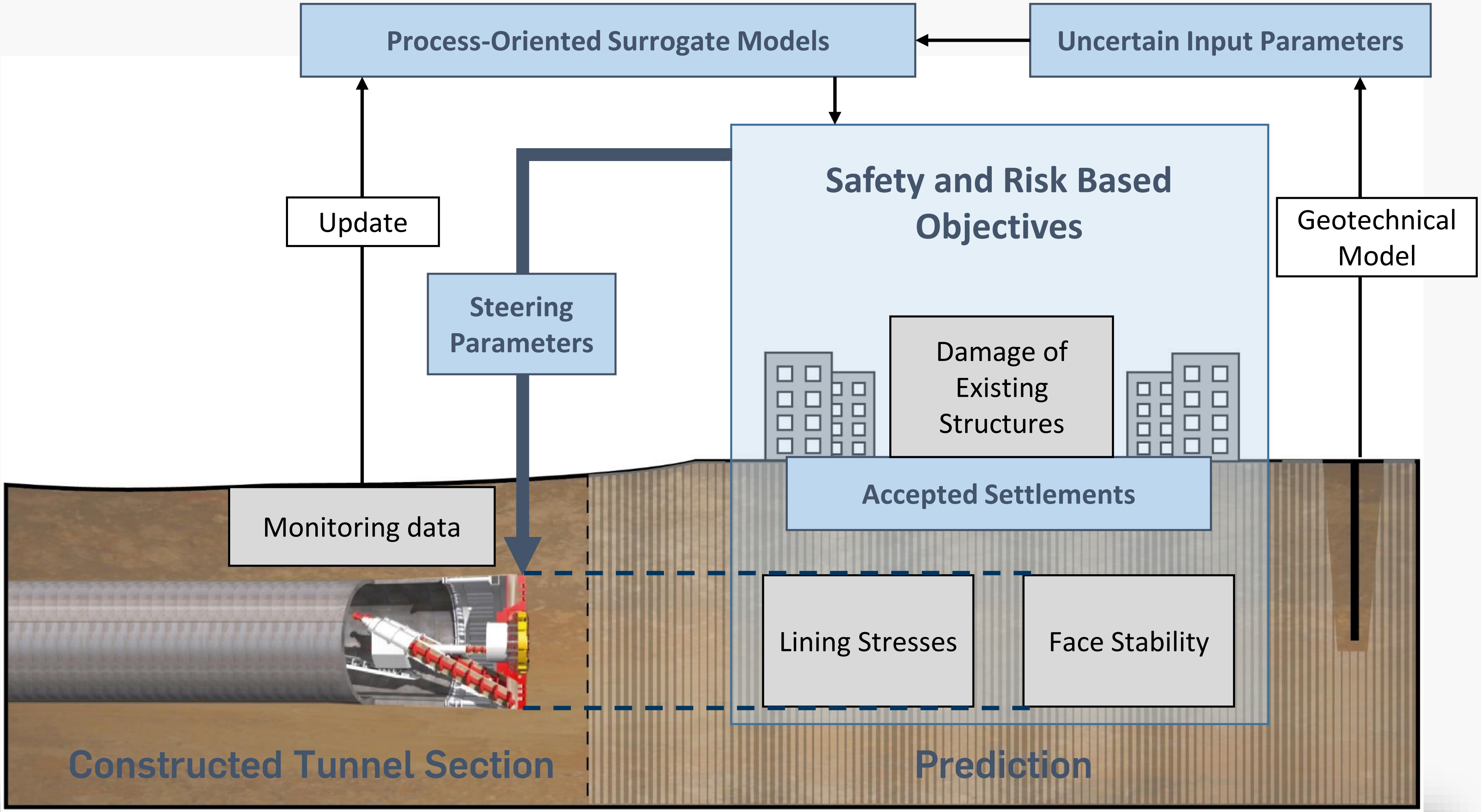
Process-Oriented Surrogate Models
Uncertain Input Parameters
Update
Steering Parameters
Safety and Risk Based Objectives
Geotechnical Model
Damage of Existing Structures
Accepted Settlements
Monitoring data
Lining Stresses
Face Stability
Constructed Tunnel Section
Prediction

FE Model for Mechanised Tunnelling

Subsystem I:
geology,
geotechnical model

Subsystem II:
face support

Subsystem III:
soil excavation

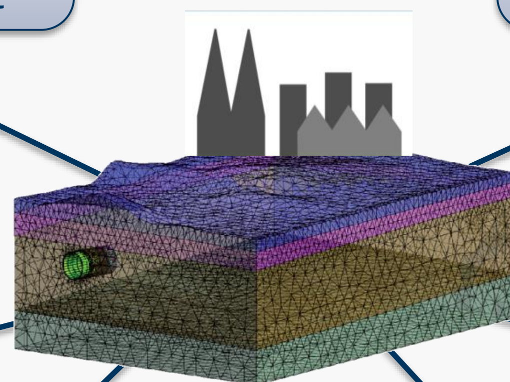

Subsystem IV:
tunnel boring machine,
steering

Subsystem VI:
existing buildings

Subsystem V:
lining

FE Model for Mechanised Tunnelling

simplified models for buildings

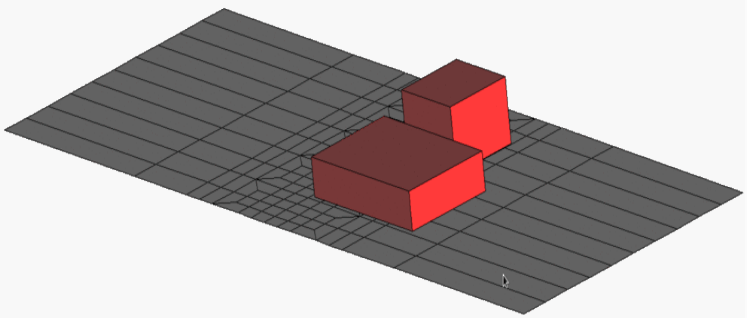

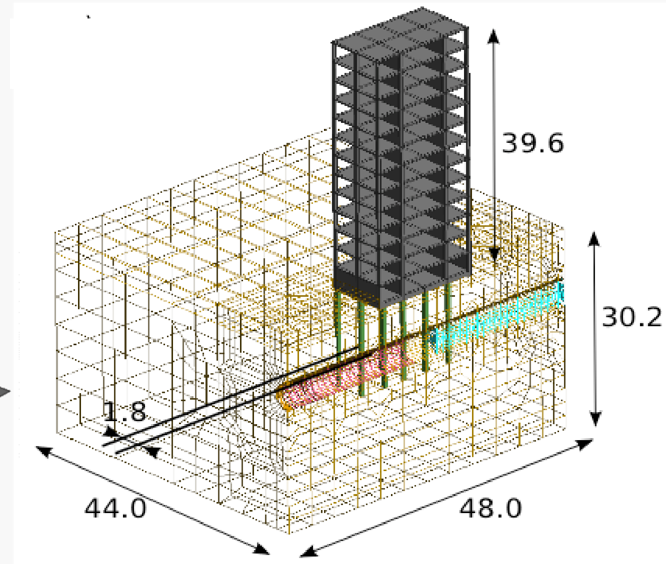

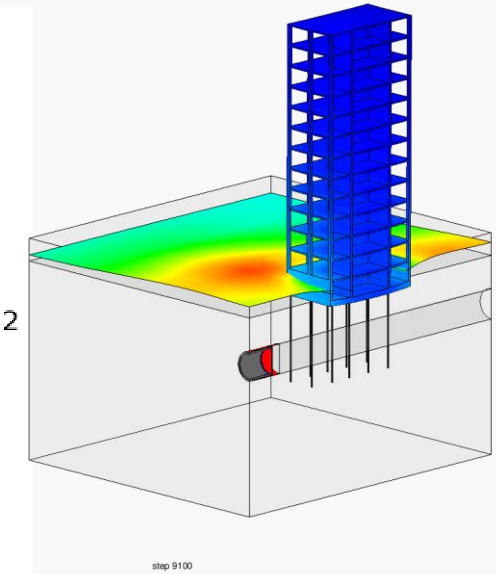

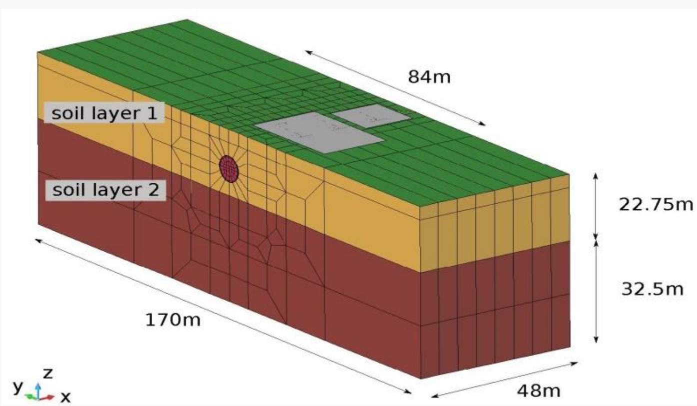

Embedded beam element for pile foundation

- independent of the soil mesh
- arbitrary number and orientation per element
- skin friction, pile tip resistance

J. Ninić, J. Stascheit & G. Meschke, Int. J. Num. Anal. Meth. Geomechanics, 2013

FE Model for Mechanised Tunnelling

Computational models

advanced finite element simulation

- a priori – tunnel design
- during construction – steering

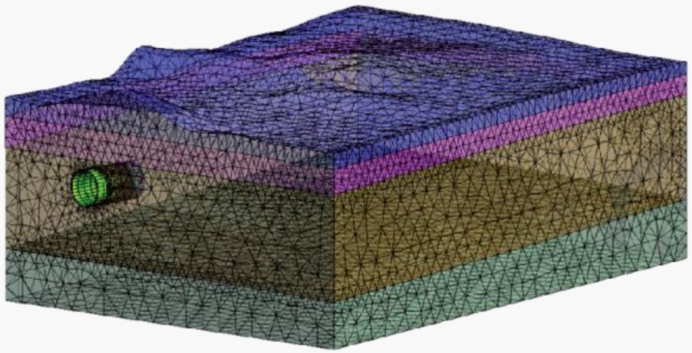

FE Model for Mechanised Tunnelling

Computational models

advanced finite element simulation

- a priori – tunnel design
- during construction – steering

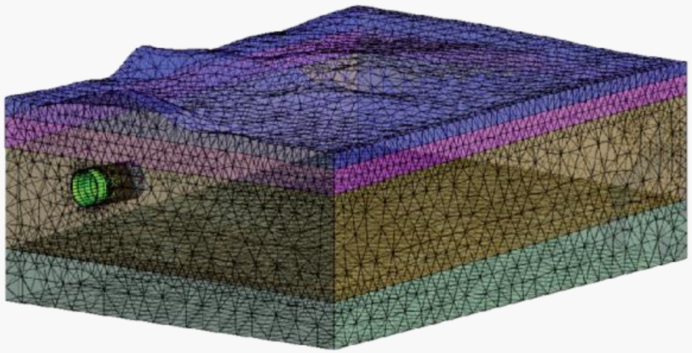

Uncertainties

limited information

- geometry and heterogeneity of soil layers
- construction process

} uncertain parameters

Polymorphic Uncertainty Modelling

aleatory

- randomness / variability
- not reducible
- objective assessment

↓

stochastic numbers

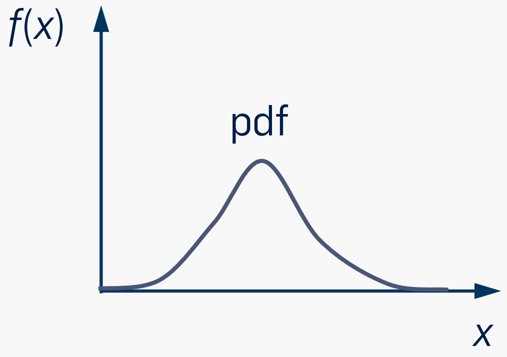

Polymorphic Uncertainty Modelling

aleatory

- randomness / variability
- not reducible
- objective assessment

↓

stochastic numbers

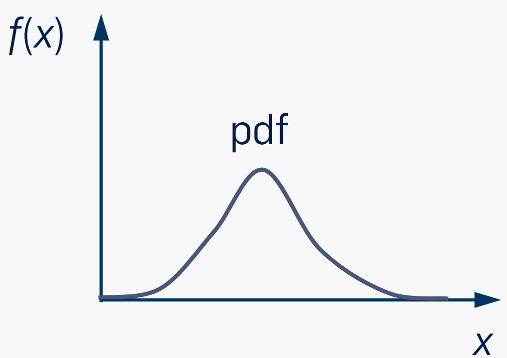

epistemic

- lack of knowledge
- reducible
- subjective / objective assessment

↓

intervals, fuzzy numbers

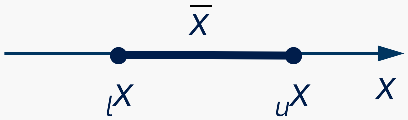

Geotechnical parameter	Range
Young's Modulus E_1 [MPa]	10 – 30
Friction angle φ_1 [°]	25 – 35

Polymorphic Uncertainty Modelling

Generalized uncertainty models

probability boxes

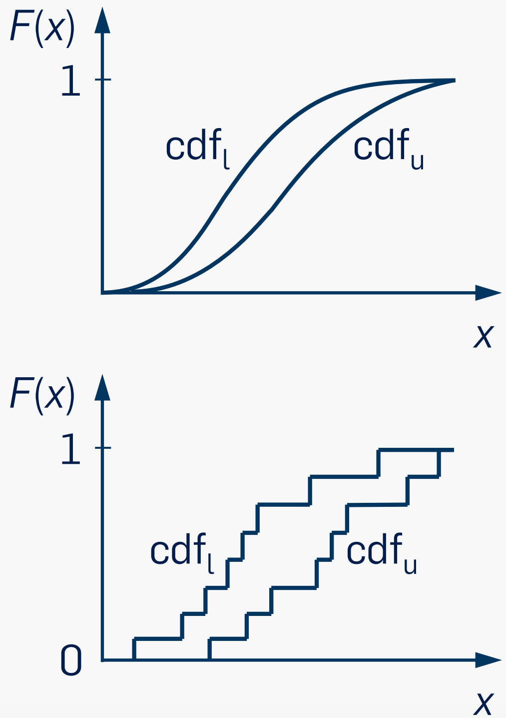

fuzzy stochastic numbers

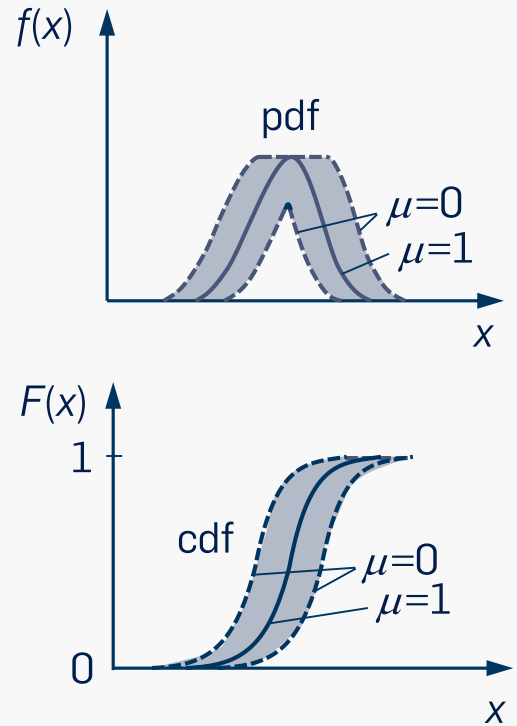

Computing with Interval Data

Mapping of processes with interval parameters

- Type 1 Mapping

geotechnical parameters $\bar{X}$

steering parameters $P(t)$

$\longrightarrow$ $\bar{S}(t)$ time variant interval settlement field

Computing with Interval Data

Mapping of processes with interval parameters

- Type 1 Mapping

geotechnical parameters $\bar{X}$
steering parameters $P(t)$ $\longrightarrow$ $\bar{S}(t)$ time variant interval settlement field

- Type 2 Mapping

steering parameters $P(t)$ $\overline{\longrightarrow}$ $\bar{S}(t)$ time variant interval settlement field

Computing with Interval Data

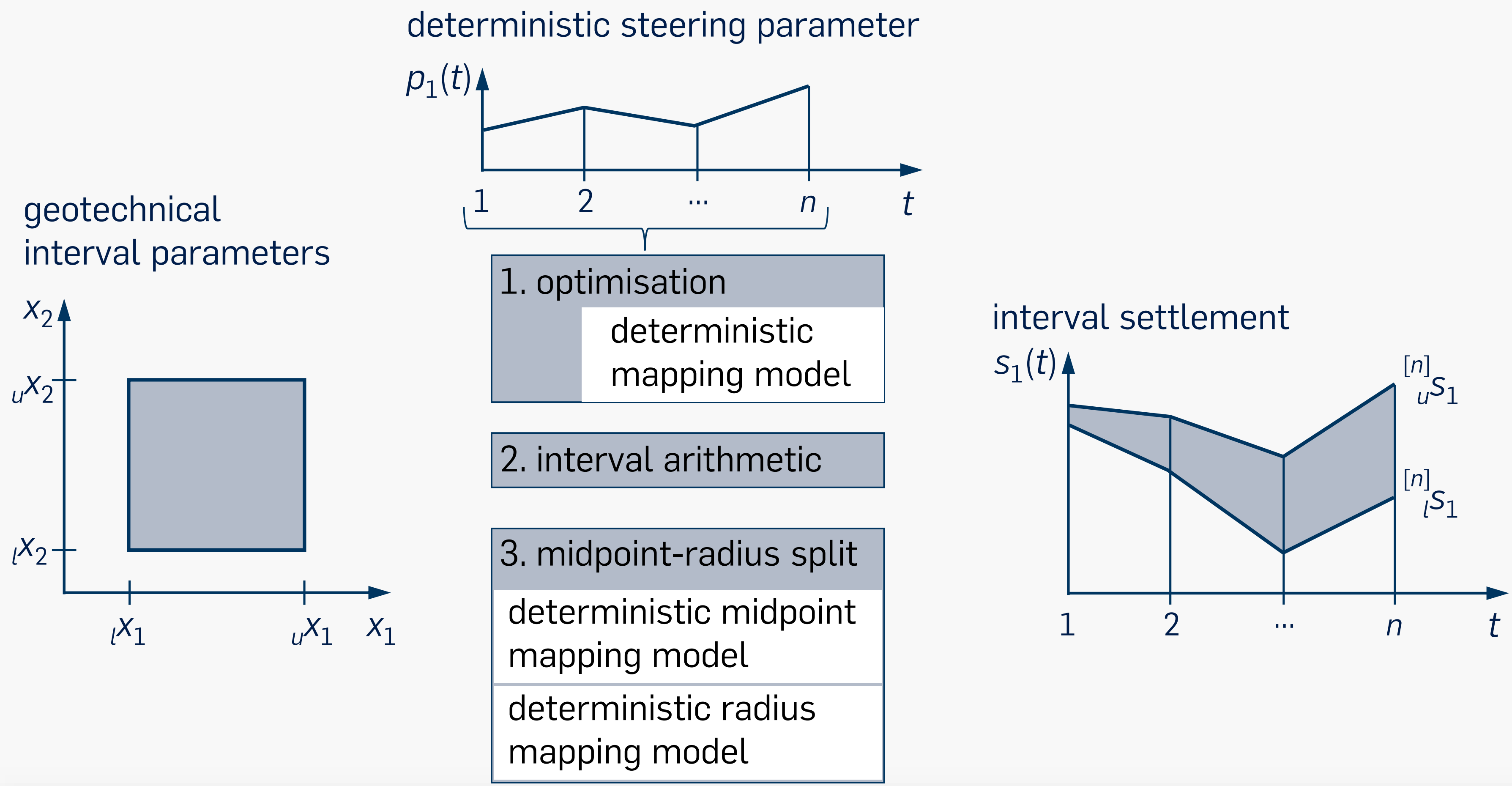

S. Freitag, B.T. Cao, J. Ninić & G. Meschke, Computers & Structures, submitted

Computing with Interval Data

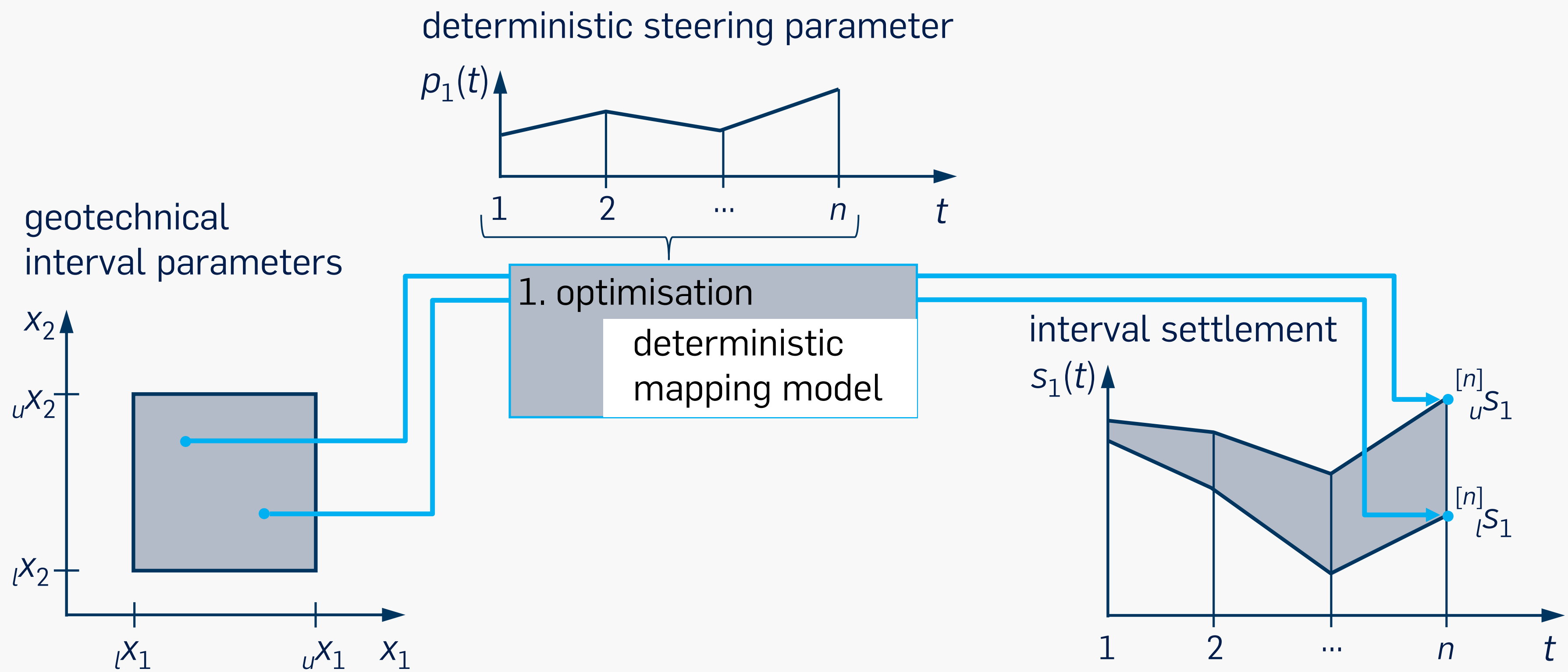

S. Freitag, B.T. Cao, J. Ninić & G. Meschke, Computers & Structures, submitted

Computing with Interval Data

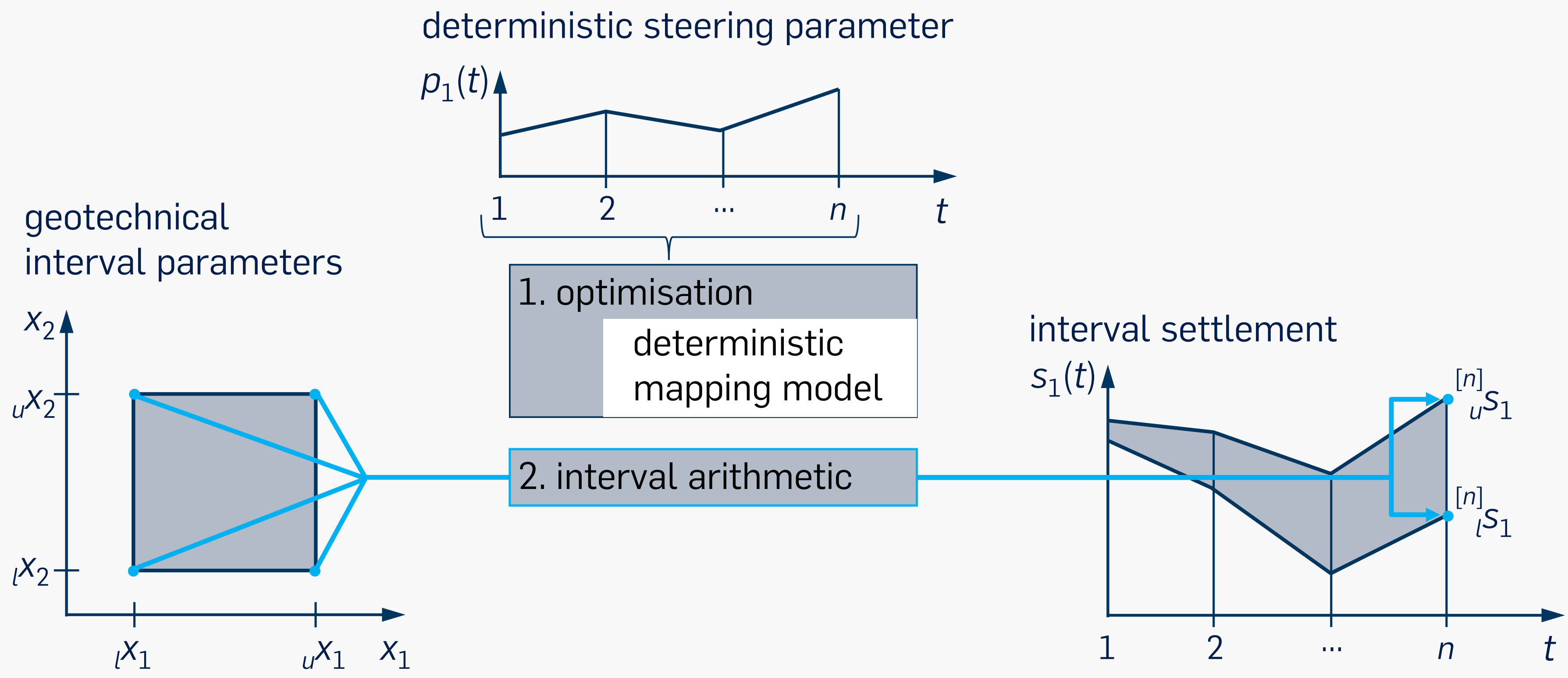

S. Freitag, B.T. Cao, J. Ninić & G. Meschke, Computers & Structures, submitted

Computing with Interval Data

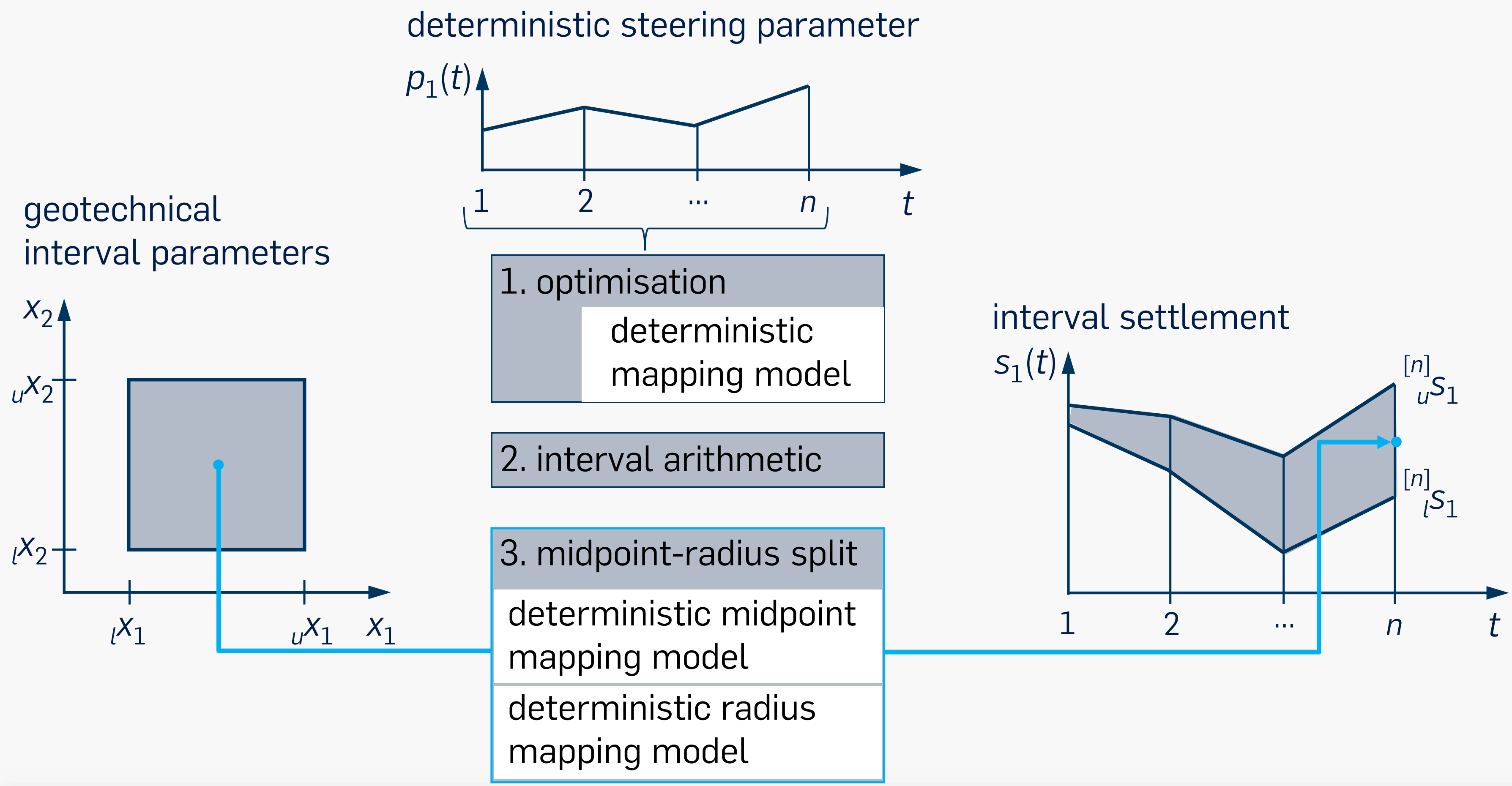

S. Freitag, B.T. Cao, J. Ninić & G. Meschke, Computers & Structures, submitted

Computing with Interval Data

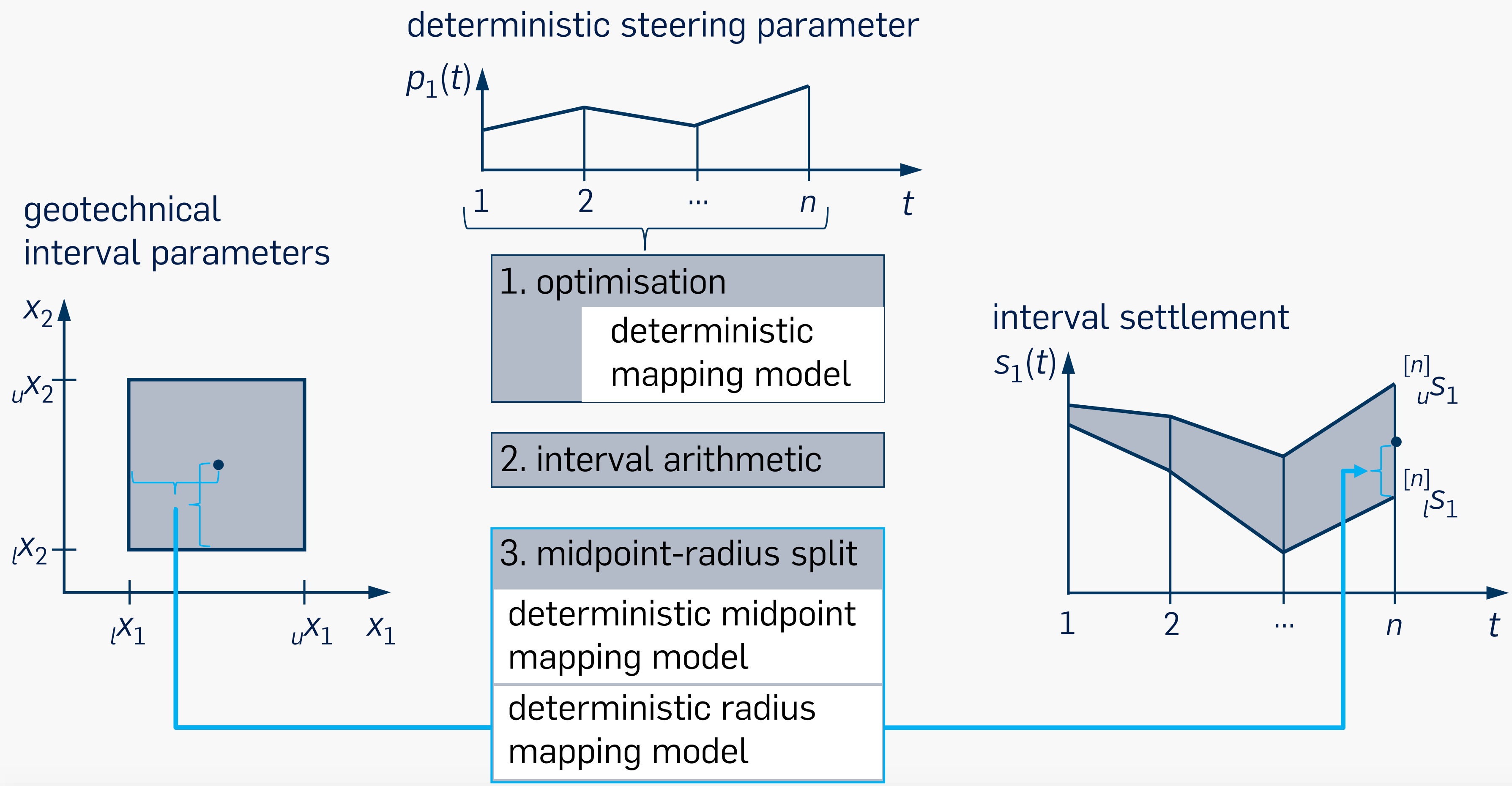

S. Freitag, B.T. Cao, J. Ninić & G. Meschke, Computers & Structures, submitted

Computing with Interval Data

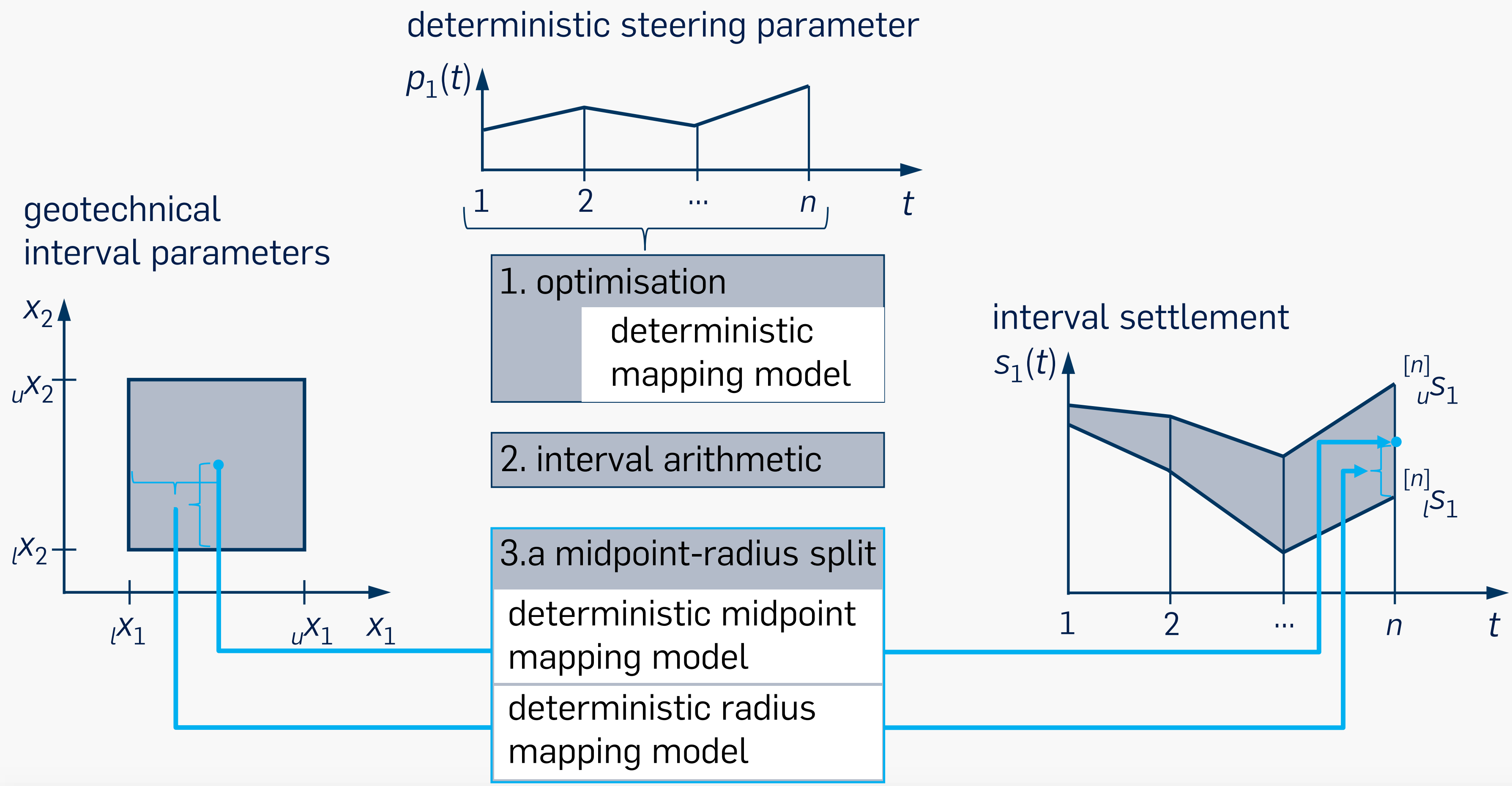

S. Freitag, B.T. Cao, J. Ninić & G. Meschke, Computers & Structures, submitted

Computing with Interval Data

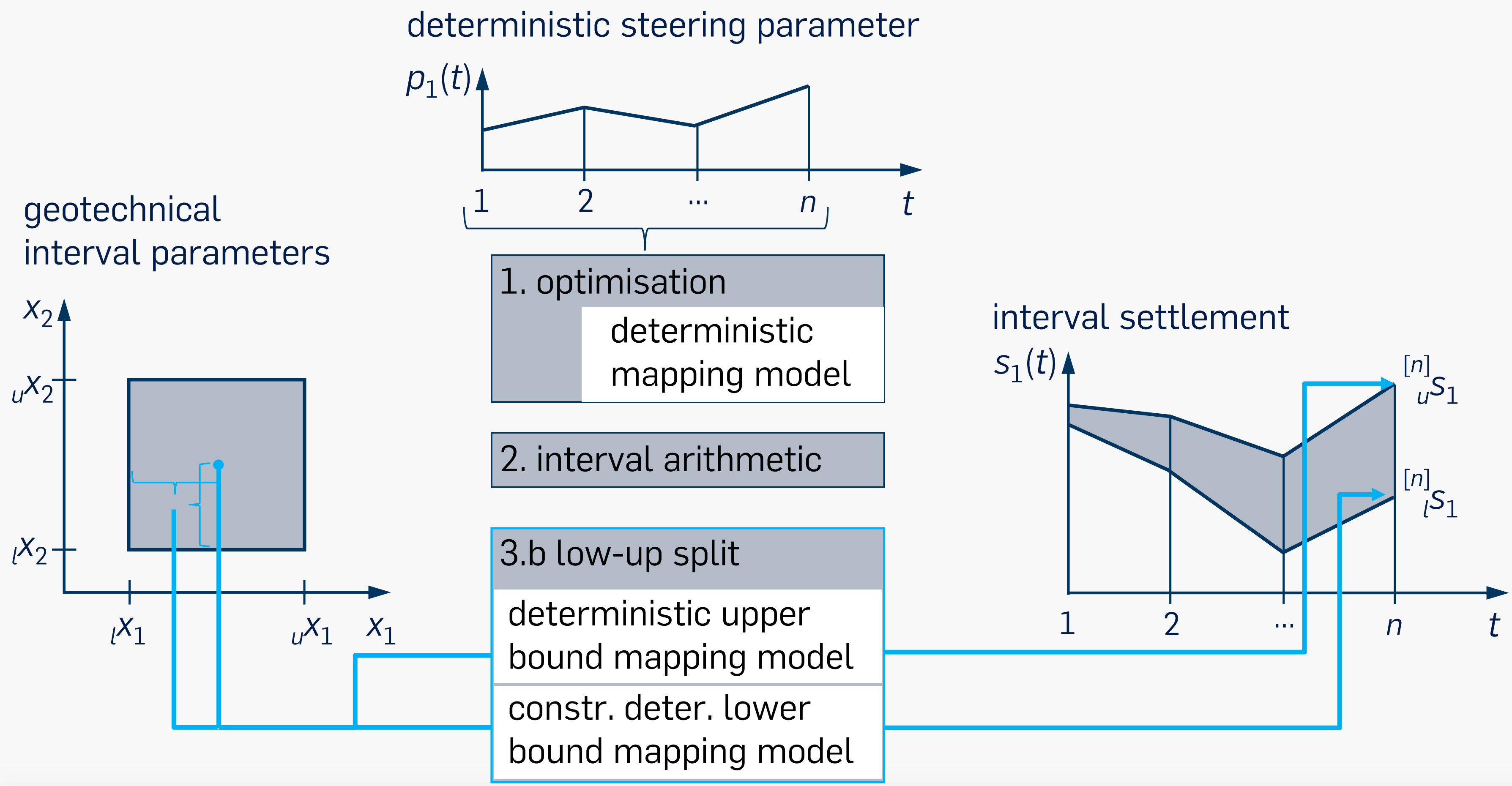

Hybrid RNN-GPOD Surrogate Model

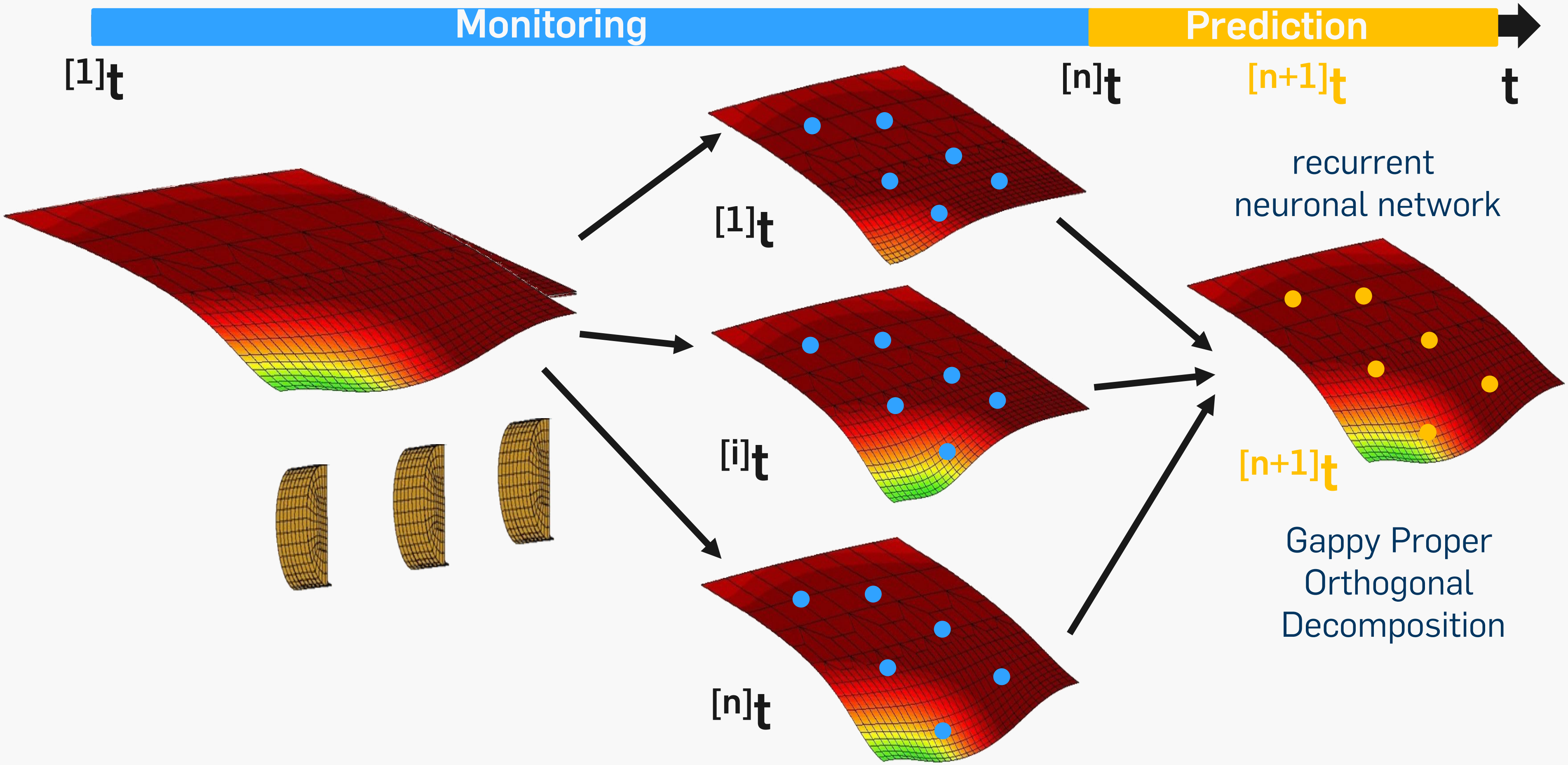

B.T. Cao, S. Freitag & G. Meschke, Advanced Modeling and Simulation in Engineering Sciences, 2016

Hybrid RNN-GPOD Surrogate Model

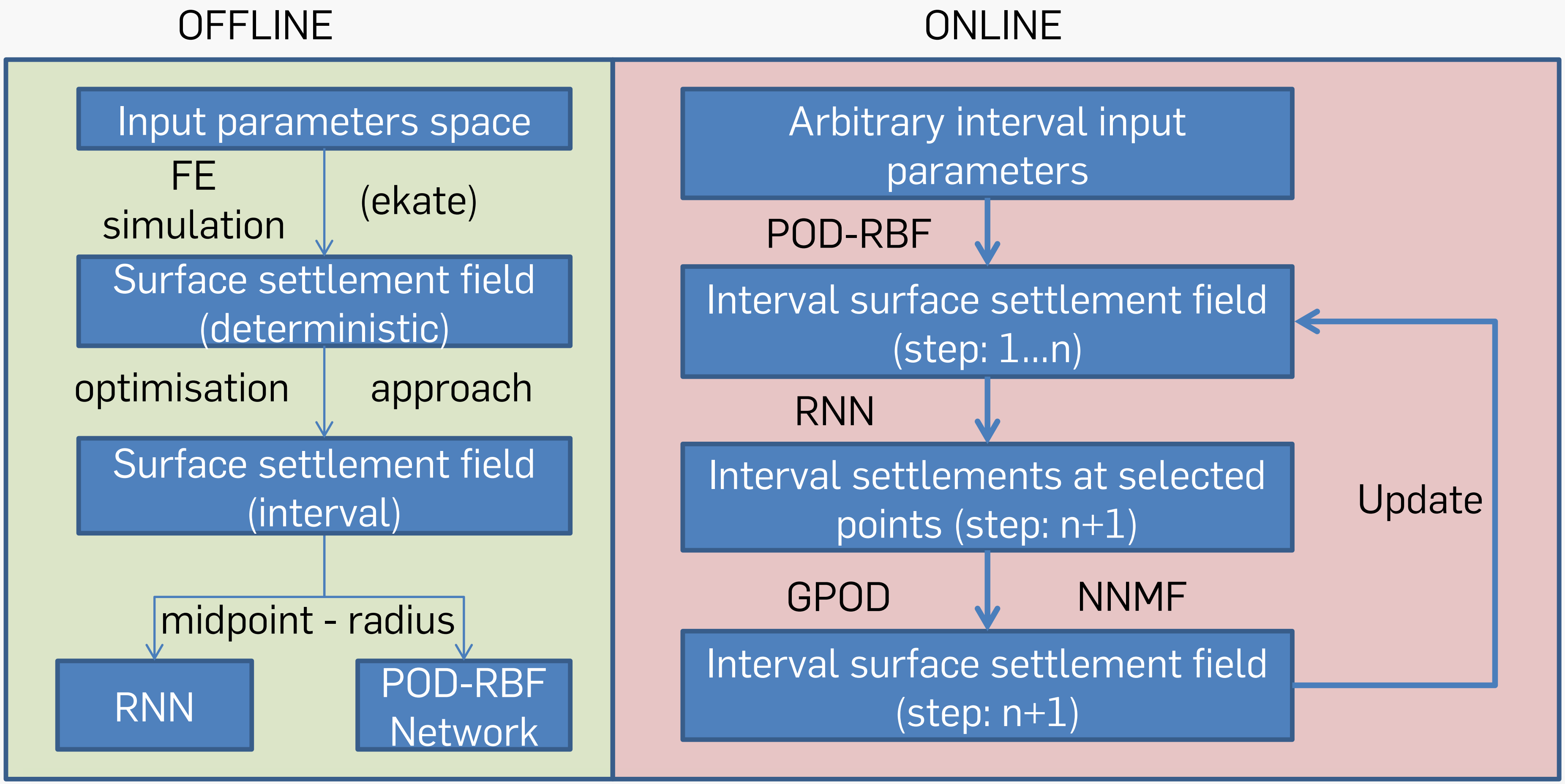

Recurrent Neural Network

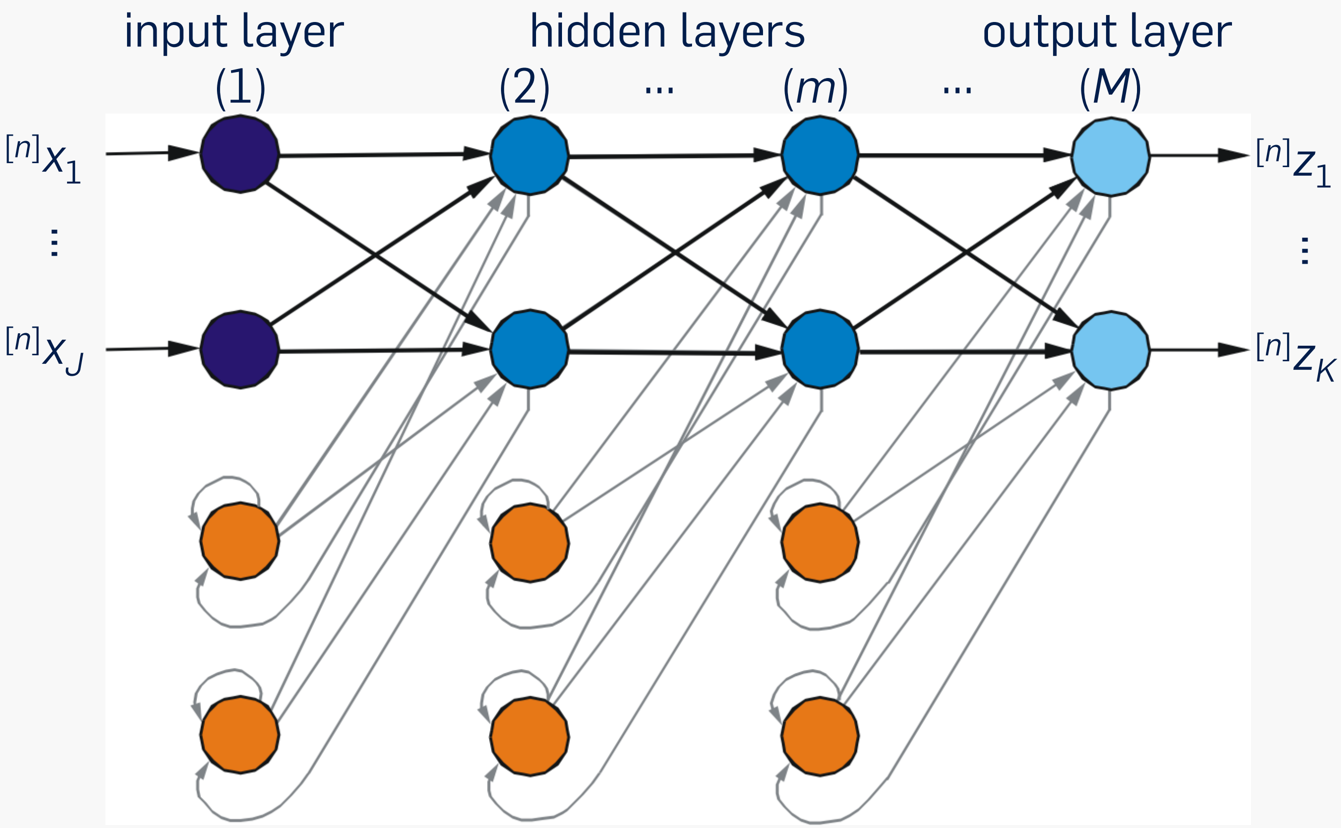

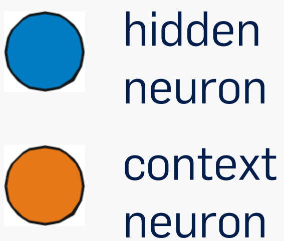

Recurrent Neural Network

- hidden neuron

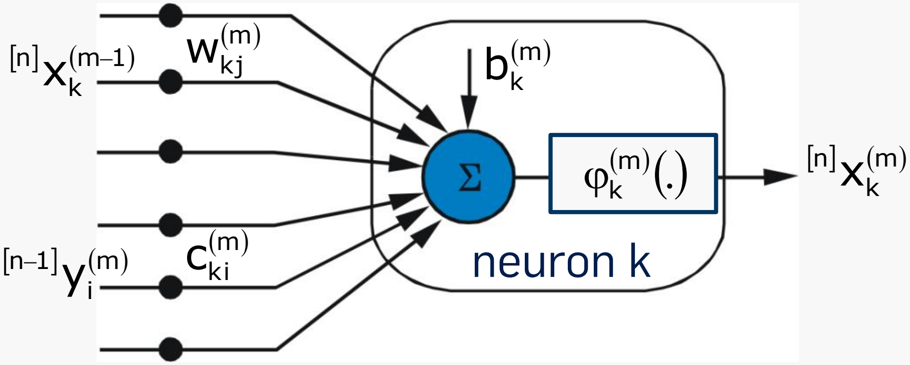

$$^{[n]}x_k^{(m)} = \varphi_k^{(m)}\left(\sum_{j=1}^{J^{(m-1)}} \left[{}^{[n]}x_j^{(m-1)} \cdot w_{kj}^{(m)} \right] + b_k^{(m)} + \sum_{i=1}^{I^{(m)}} \left[{}^{[n-1]}y_i^{(m)} \cdot c_{ki}^{(m)} \right] \right)$$

Recurrent Neural Network

- hidden neuron

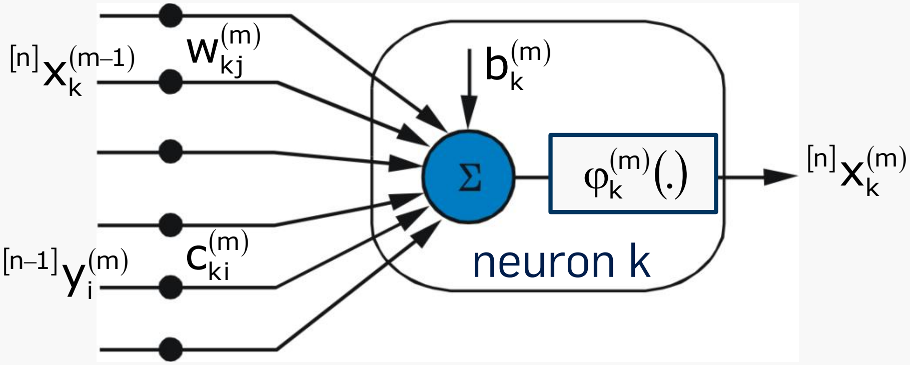

$$^{[n]}x_k^{(m)} = \varphi_k^{(m)}\left(\sum_{j=1}^{J^{(m-1)}} \left[^{[n]}x_j^{(m-1)} \cdot w_{kj}^{(m)} \right] + b_k^{(m)} + \sum_{i=1}^{I^{(m)}} \left[^{[n-1]}y_i^{(m)} \cdot c_{ki}^{(m)} \right] \right)$$

- context neuron

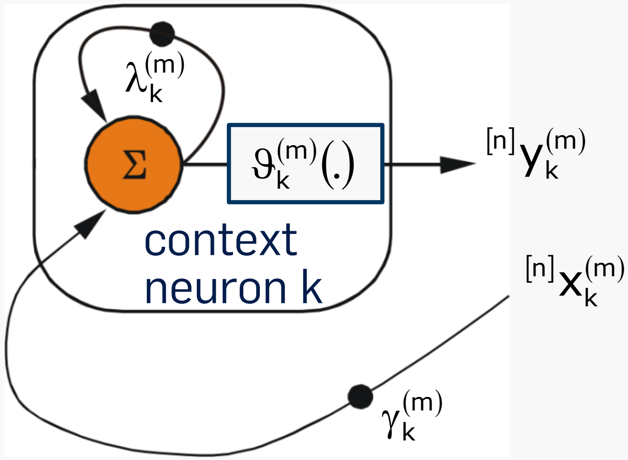

$$^{[n]}y_k^{(m)} = \vartheta_k^{(m)}\left(^{[n]}x_k^{(m)} \cdot \gamma_k^{(m)} + {}^{[n-1]}y_k^{(m)} \cdot \lambda_k^{(m)} \right)$$

Gappy Proper Orthogonal Decomposition

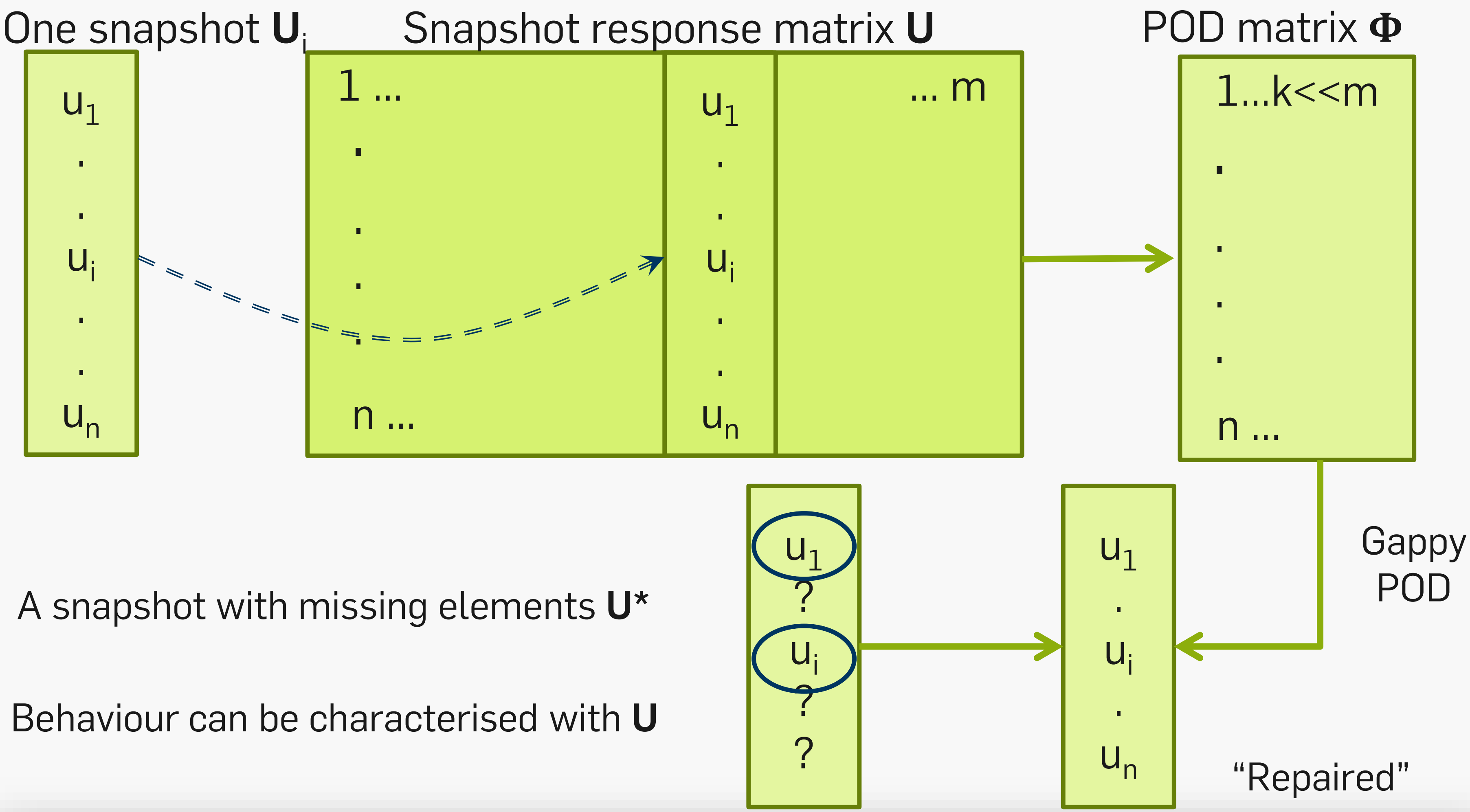

GPOD and Non-Negative Matrix Factorization

	GPOD	NNMF
Matrix approx.	${}_mS \approx \hat{\Phi} \cdot \hat{A}$	${}_rS \approx W \cdot H$
Basis vectors	$\hat{\Phi}$	W
Min. problem	$min. \left\| {}^*S - \hat{\Phi} \cdot {}^*A \right\|_n^2$	$min. \left\| {}^+S - W \cdot {}^+H \right\|_n^2$
Constraint	unconstrained	$W, {}^+H \geq 0$
Solution	${}_mM \cdot {}^*A = {}_mR$ ${}_mM = (\hat{\Phi}^T, \hat{\Phi})$ ${}_mR = (\hat{\Phi}^T, {}^*S)$	${}_rM \cdot {}^+H = {}_rR$ ${}_rM = (W^T, W)$ ${}_rR = (W^T, {}^+S)$
	Linear least square	Non-negative linear least square

Constrained GPOD

	Unconstrained GPOD	Constrained GPOD
Matrix approx.	${}_uS \approx {}_u\widehat{\Phi} \cdot {}_u\hat{A}$	${}_lS \approx {}_l\widehat{\Phi} \cdot {}_l\hat{A}$
Basis vectors	${}_u\widehat{\Phi}$	${}_l\widehat{\Phi}$
Min. problem	$min. \left\Vert {}_u^*S - {}_u\widehat{\Phi} \cdot {}_u^*\widehat{\boldsymbol{A}} \right\Vert_n^2$	$min. \left\Vert {}_l^*S - {}_l\widehat{\Phi} \cdot {}_l^*\widehat{\boldsymbol{A}} \right\Vert_n^2$
Constraint	unconstrained	${}_l\widehat{\Phi} \cdot {}_l^*\widehat{\boldsymbol{A}} < {}_uS$
Solution	${}_uM \cdot {}_u^*\widehat{\boldsymbol{A}} = {}_uR$ ${}_uM = ({}_u\widehat{\Phi}^T, {}_u\widehat{\Phi})$ ${}_uR = ({}_u\widehat{\Phi}^T, {}_u^*S)$	${}_lM \cdot {}_l^*\widehat{\boldsymbol{A}} \approx {}_lR$ ${}_lM = ({}_l\widehat{\Phi}^T, {}_l\widehat{\Phi})$ ${}_lR = ({}_l\widehat{\Phi}^T, {}_l^*S)$
	Linear least square (lsq)	Linear lsq with inequality constraint

Verification Example

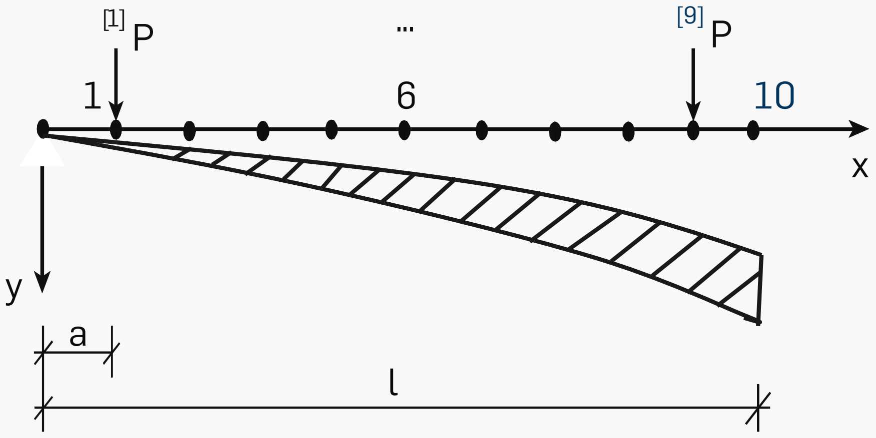

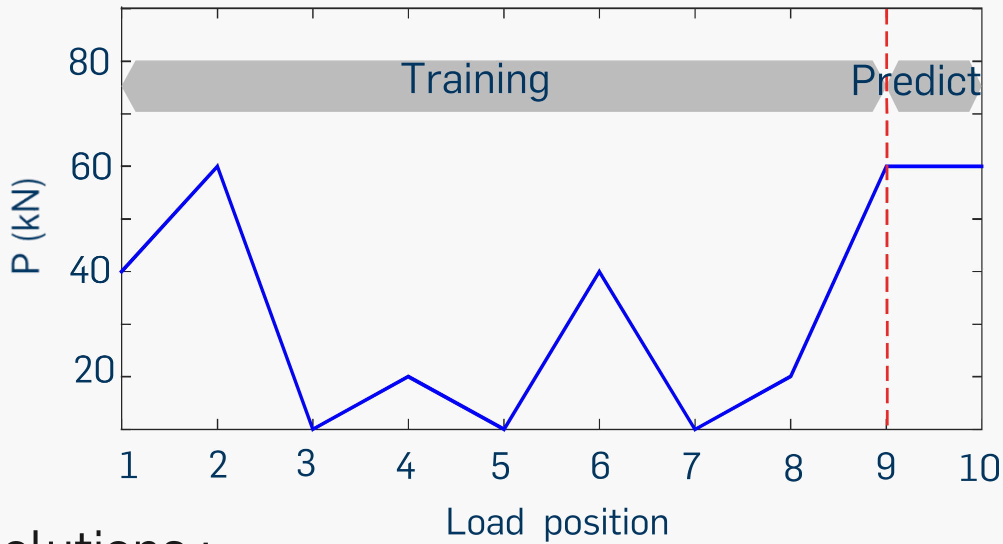

$\bar{E}$ = [30,36] GPa

I = 0.01 m^4

l = 10 m

11 nodes

10 load positions

Analytical solutions :

$$\bar{S}(x) = \frac{Px^2}{6\bar{E}I}(3l - x), \qquad for\ 0 < x < a$$

$$\bar{S}(x) = \frac{Pl^2}{6\bar{E}I}(3x - l), \qquad for\ a < x < l$$

Verification Example

1600 snapshots (8 $\bar{E}$ x 200 scenarios of *P(t)*)

Mid-rad matrix

$$_{mr}S = \begin{bmatrix} [0,0] & \dots & [0,0] & \dots & [0,0] \\ [0.017,0.003] & \dots & [0.066,0.015] & \dots & [0.855,0.082] \\ \dots & & \dots & & \dots \\ [0.242,0.048] & \dots & [2.926,0.671] & \dots & [55.95,5.357] \end{bmatrix}$$

Up-low matrix

$$_{ul}S = \begin{bmatrix} [0,0] & \dots & [0,0] & \dots & [0,0] \\ [0.014,0.020] & \dots & [0.051,0.081] & \dots & [0.773,0.937] \\ \dots & & \dots & & \dots \\ [0.194,0.290] & \dots & [2.255,3.597] & \dots & [50.593,61.307] \end{bmatrix}$$

9 steps of *P(t)*

Reduced bases W, $_m\hat{\Phi}$, $_u\hat{\Phi}$ and $_l\hat{\Phi}$

$$W = \begin{bmatrix} 0 & 0 \\ 0.01 & 0.02 \\ 0.03 & 0.08 \\ \dots & \dots \\ 0.49 & 0.36 \\ 0.58 & 0.32 \end{bmatrix} \quad {}_m\hat{\Phi} = \begin{bmatrix} 0 & 0 \\ 0.009 & 0.053 \\ 0.034 & 0.173 \\ \dots & \dots \\ 0.500 & -0.209 \\ 0.583 & -0.470 \end{bmatrix} \quad {}_u\hat{\Phi} = \begin{bmatrix} 0 & 0 \\ 0.009 & 0.052 \\ 0.034 & 0.170 \\ \dots & \dots \\ 0.500 & -0.209 \\ 0.583 & -0.471 \end{bmatrix} \quad {}_l\hat{\Phi} = \begin{bmatrix} 0 & 0 \\ 0.009 & 0.054 \\ 0.034 & 0.175 \\ \dots & \dots \\ 0.500 & -0.209 \\ 0.583 & -0.469 \end{bmatrix}$$

11 nodes

Verification Example

- Prediction at nodes 2, 6 and 10 (RNNs)

$$ {}^{RNN}_{m}S = \begin{bmatrix} 0.8795 \\ 19.310 \\ 52.365 \end{bmatrix} \quad {}^{RNN}_{r}S = \begin{bmatrix} 0.0795 \\ 0.2243 \\ 4.635 \end{bmatrix} \quad {}^{RNN}\bar{S} = \begin{bmatrix} [0.800, 0.959] \\ [17.607, 21.013] \\ [47.730, 57.000] \end{bmatrix} \quad {}^{an}\bar{S} = \begin{bmatrix} [0.806, 0.967] \\ [17.361, 20.833] \\ [47.250, 56.700] \end{bmatrix} $$

Errors: 0.58% and 1.07% for lower and upper bounds

- Prediction at other nodes (GPOD and NNMF)

$$ S^* = \begin{bmatrix} ? \\ [0.800, 0.959] \\ \dots\dots \\ ? \\ [17.607, 21.013] \\ ? \\ \dots\dots \\ [47.730\ 57.000] \\ ? \end{bmatrix} \quad {}_{ul}S^* = \begin{bmatrix} [0.000, 0.000] \\ [\mathbf{0.800}, \mathbf{0.959}] \\ \dots\dots \\ [11.689, 13.949] \\ [\mathbf{17.607}, \mathbf{21.013}] \\ [24.373, 29.093] \\ \dots\dots \\ [\mathbf{47.730}\ \mathbf{57.000}] \\ [55.840, 66.689] \end{bmatrix} \quad {}_{mr}S^* = \begin{bmatrix} [0.000, 0.000] \\ [\mathbf{0.800}, \mathbf{0.959}] \\ \dots\dots \\ [11.590, 14.047] \\ [\mathbf{17.607}, \mathbf{21.013}] \\ [24.422, 29.043] \\ \dots\dots \\ [\mathbf{47.730}\ \mathbf{57.000}] \\ [55.804, 66.725] \end{bmatrix} \quad {}^{an}S = \begin{bmatrix} [0.000, 0.000] \\ [\mathbf{0.806}, \mathbf{0.967}] \\ \dots\dots \\ [11.556, 13.867] \\ [\mathbf{17.361}, \mathbf{20.833}] \\ [24.000, 28.800] \\ \dots\dots \\ [\mathbf{47.250}, \mathbf{56.700}] \\ [55.556, 66.667] \end{bmatrix} $$

Verification Example

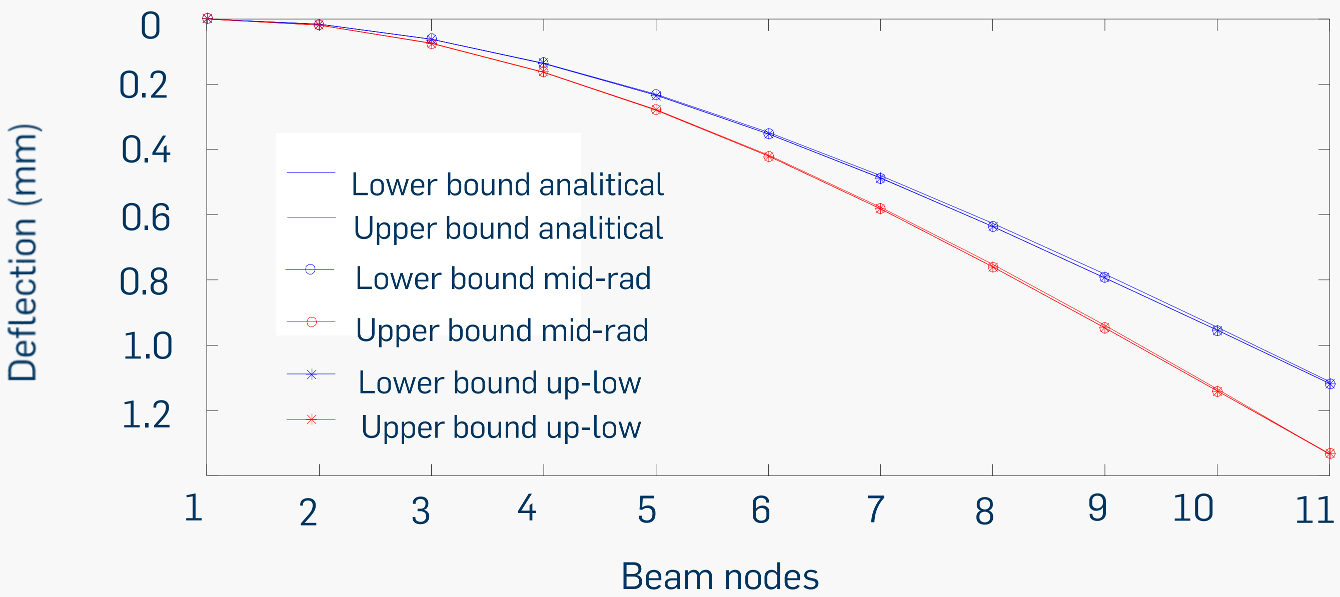

Mid-rad		Up-low	
Lower bound	Upper bound	Lower bound	Upper bound
1.18	0.61	1.09	0.34

Verification Example

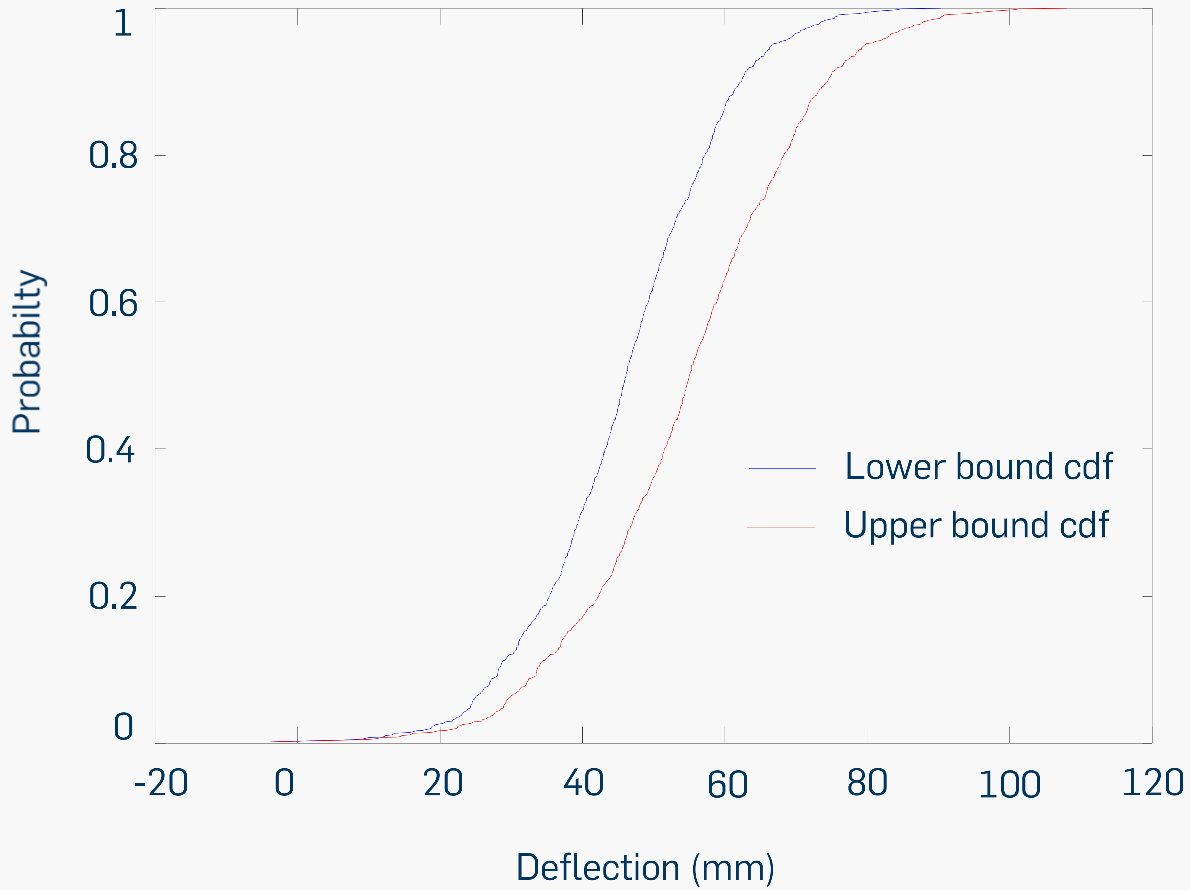

$\bar{E}$ = [30,36] Gpa

1000 samples
P: Gaussian distribution
Mean value : 50 kN
Standard deviation σ = 15 kN

Computation time
Surrogate model: 0.5h
Optimization: 10h

P-box for the deflection of the cantilever beam at node 11 for time step 10

Application Example

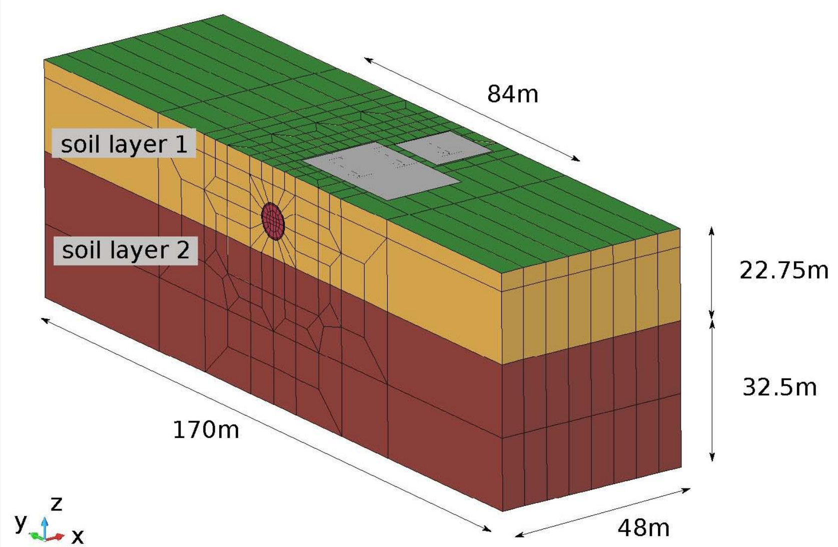

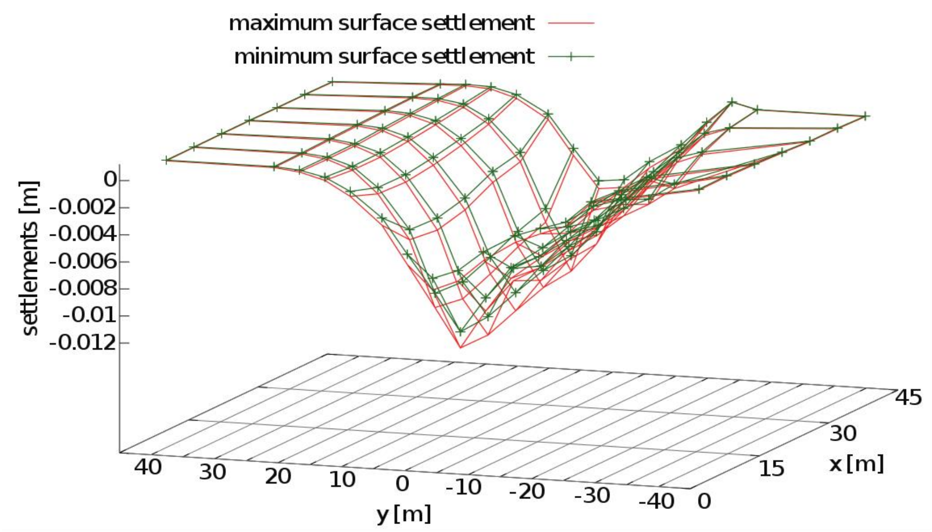

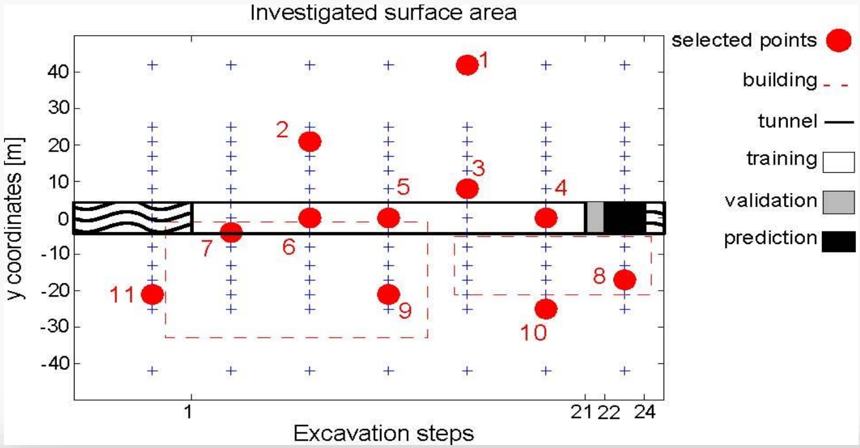

Mid-rad		Up-low	
LB	UB	LB	UB
6.2	8.9	5.9	8.0

Computation time

Surrogate model: 2s
Optimization: 1.5h

Application Example

- Real-time steering support in mechanised tunnelling

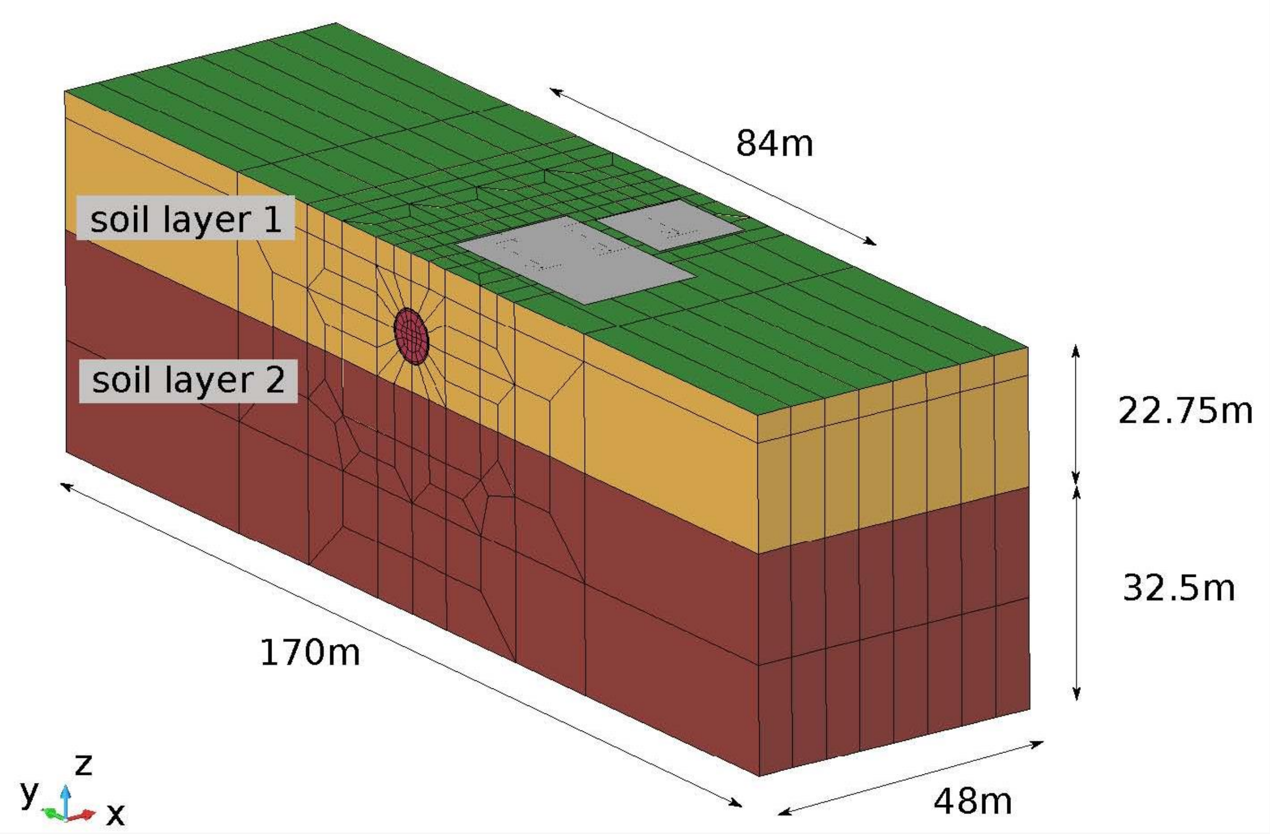

Conclusion / Outlook

Conclusion

- FE simulations for mechanised tunnelling processes
- Hybrid RNN-GPOD based surrogate model
- Real-time prediction of interval settlement fields with mid-rad and up-low representations of interval input-output data

Conclusion / Outlook

Conclusion

- FE simulations for mechanised tunnelling processes
- Hybrid RNN-GPOD based surrogate model
- Real-time prediction of interval settlement fields with mid-rad and up-low representations of interval input-output data

Outlook

- Extension for fuzzy data and polymorphic uncertainty
- Additional steering objectives: face stability, lining forces, damage risk of existing buildings
- Integration of monitoring data and application project

Thank you very much for your attention !